Published in final edited form as:
Circulation. 2010 January 5; 121(1): 26. doi:10.1161/CIRCULATIONAHA.109.865568.

Brain Volume and Metabolism in Fetuses with Congenital Heart Disease: Evaluation with Quantitative Magnetic Resonance Imaging and Spectroscopy

Catherine Limperopoulos, PhD[a,b], **Wayne Tworetzky, MD**[c], **Doff B. McElhinney, MD**[c], **Jane W. Newburger, MD MPH**[c], **David W. Brown, MD**[c], **Richard L. Robertson Jr, MD**[d], **Nicolas Guizard, MEng**[a], **Ellen McGrath, BSc RN**[c], **Judith Geva, MSW**[c], **David Annese, RT(R)**[c], **Carolyn Dunbar-Masterson, BSc RN**[c], **Bethany Trainor, BSc RN**[c], **Peter C. Laussen, MD**[e], and **Adré J. du Plessis, MBChB, MPH**[b]

[a]Department of Neurology and Neurosurgery, McGill University, Montreal, Quebec, Canada

[b]Fetal-Neonatal Neurology Research Group, Department of Neurology, Children's Hospital Boston and Harvard Medical School; Boston, Massachusetts

[c]Department of Cardiology and Pediatrics, Children's Hospital Boston and Harvard Medical School; Boston, Massachusetts

[d]Department of Radiology, Children's Hospital Boston and Harvard Medical School; Boston, Massachusetts

[e]Department of Cardiology and Anaesthesia, Children's Hospital Boston and Harvard Medical School; Boston, Massachusetts

Abstract

Background—Adverse neurodevelopmental outcome is an important source of morbidity in children with congenital heart disease (CHD). A significant proportion of newborns with complex CHD have abnormalities of brain size, structure, and/or function, suggesting that antenatal factors may contribute to childhood neurodevelopmental morbidity.

Methods and Results—Brain volume and metabolism were compared prospectively between 55 fetuses with CHD and 50 normal fetuses using 3-D volumetric magnetic resonance imaging (MRI) and magnetic resonance spectroscopy (^{1}H-MRS). Fetal intracranial cavity (ICV), cerebrospinal fluid, and total brain volumes (TBV) were measured by manual segmentation. ^{1}H-MRS was used to measure the cerebral N-acetyl aspartate:choline ratio (NAA:Cho) and identify cerebral lactate. Complete fetal echocardiograms were performed. Gestational age (GA) at MRI ranged from 25 1/7 to 37 1/7 weeks (median 30 weeks). During the third trimester, there were progressive and significant declines in GA-adjusted TBV and ICV in CHD fetuses relative to controls. NAA:Cho increased progressively over the third trimester in normal fetuses, but the rate of rise was significantly slower ($p<0.001$) in CHD fetuses. On multivariable analysis adjusting for GA and weight percentile, cardiac diagnosis and percentage of combined ventricular output through the aortic valve were independently associated with TBV. Independent predictors of lower NAA:Cho included diagnosis, absence of antegrade aortic arch flow, and evidence of cerebral lactate ($p<0.001$).

Corresponding author: Catherine Limperopoulos, Montreal Children's Hospital, Pediatric Neurology, 2300 Tupper Street A-334, Montreal, Quebec, H3H 1P3, Phone: 514-412-4400 (22184), Fax: 514-412-4373, catherine.limperopoulos@mcgill.ca.

Conflict of Interest Disclosures: **None.**

Conclusions—Third-trimester fetuses with some forms of CHD have smaller GA- and weight-adjusted TBV than normal fetuses, and evidence of impaired neuroaxonal development and metabolism. Hemodynamic factors may play an important role in this abnormal development.

Keywords

brain; magnetic resonance imaging; pediatrics; congenital; fetal

Introduction

Neurologic and developmental dysfunction are among the most common extracardiac complications in children with complex congenital heart disease (CHD) [1-4]. Cerebral perfusion abnormalities that occur during intraoperative cardiopulmonary support may cause neurologic injury, and extensive research has been performed on the impact of perioperative management on neurodevelopmental outcomes [5-8]. However, there is increasing evidence that adverse neurodevelopmental outcomes in children with complex CHD are due not only perioperative insult, but to inborn factors as well. Reports from a number of investigators have documented a high prevalence of anatomic and functional neurologic abnormalities prior to surgery in newborns with CHD [9-17], and an association of such abnormalities with childhood developmental status [11,13,18,19]. These findings support the hypothesis that abnormal brain development and growth in utero contribute to adverse neurodevelopmental outcomes in children with CHD.

The underlying causes of abnormal prenatal brain development in fetuses with CHD are not known, and may include both genetic and epigenetic factors. Several studies have documented abnormal cerebral blood flow in fetuses and newborns with complex anomalies such as hypoplastic left heart syndrome (HLHS) [12,20,21]. Whether these hemodynamic abnormalities are primary or secondary, it is possible that one of the factors contributing to impaired brain development in fetuses with CHD is inability of the abnormal fetal cardiovascular system to meet the metabolic demands of accelerated third-trimester brain growth and maturation.

The aim of this study was to compare brain growth and metabolism between normal fetuses and those with CHD using 3-D volumetric magnetic resonance imaging (MRI) and proton magnetic resonance spectroscopy (^{1}H-MRS). We hypothesized that, relative to normal controls, brain volume would be smaller and metabolic indices indicative of immaturity in third-trimester fetuses with some forms of CHD.

Methods

Subjects

Subjects were recruited prospectively into a longitudinal case-control study in which volumetric MRI and ^{1}H-MRS were performed at a single prenatal time-point, in the neonatal period prior to any cardiac surgery, and at 1 year of age. This report includes data from the prenatal evaluation.

The inception cohort included pregnant women undergoing fetal echocardiography at Children's Hospital Boston between September 2007 and April 2008. Mothers of fetuses with confirmed CHD were recruited as cases. Normal controls were recruited from healthy pregnant volunteers and from pregnancies with a normal fetal echocardiogram performed for a family history of CHD or for suspected CHD in the current pregnancy. The decision to approach a mother about participation was left to the discretion of the attending fetal echocardiographer. Exclusion criteria for both cases and controls included gestational age greater than 36

completed weeks; multiple gestation pregnancy; congenital infection; gestational diabetes; maternal contraindication to MRI; fetal ultrasound findings of dysmorphic features, dysgenetic brain lesions, or anomalies of other organ systems; prenatally documented chromosomal abnormalities; or inadequate MRI data quality due to excessive fetal motion. If structural brain anomalies were identified on fetal or neonatal MRI, the anomalies were reported, but these fetuses were not included in the analysis.

In cases, the MRI was typically scheduled on the same day as a follow-up fetal echocardiogram, usually several weeks after enrollment. In most control fetuses, the MRI was also performed several weeks after enrollment, but the echocardiogram was not repeated. Thus, the duration between the study echocardiogram and MRI was variable, and tended to be longer in controls than cases.

Written informed consent from mothers was obtained according to a protocol approved by the Children's Hospital Committee for Clinical Investigation.

Fetal Echocardiography

Complete anthropometric ultrasound and anatomic and Doppler echocardiographic studies were performed in all fetuses, and reviewed by two attending fetal echocardiographers (WT, DWB). Aortic and pulmonary arterial flows were calculated using pulsed-wave Doppler as: flow = valve area (computed from valve diameter) × velocity-time integral (area under the curve of the Doppler signal) × heart rate. Combined ventricular output was computed as the sum of aortic and pulmonary flow, and indexed to estimated fetal weight. Middle cerebral and umbilical arterial flow velocities (systolic, diastolic, and mean) were measured using pulsed-wave Doppler, and pulsatility and resistance indices were calculated. Patients were categorized by diagnosis as having hypoplastic left heart syndrome (HLHS) or variants thereof, d-transposition of the great arteries (TGA), pulmonary atresia, other cardiac diagnosis, or normal.

Estimated GA was based on maternal dates or first-trimester ultrasound measurement, if available. Fetal weight was estimated by Hadlock's formula [22], and fetal weight percentile was calculated from equations reported by Doubilet et al. [23].

Fetal Brain MRI

MRI scans were performed using a 1.5 Tesla scanner (Achiva, Philips Medical System, Netherlands) and a 5-channel phased array cardiac coil. Multiplanar single shot turbo spin echo (SSTSE) imaging was performed (TE_{eff}=120 msec, TR=12500 msec, 0.625 signal averages, 330 mm field of view, 2 mm slice thickness, no interslice gap, 256 × 204 acquisition matrix, acquisition time 30-60 seconds). ^{1}H-MRS was performed using a single voxel technique and the spectra were acquired using a point resolved echo spectroscopic (PRESS) sequence (TE=144 msec, TR=1500 msec, 64 signal averages, scan time approximately 3 minutes). Maternal sedation was not administered. The 4.5 cm^3 (20×15×15 mm^3) volume of interest was placed within the cerebral hemisphere at the level of the centrum ovale, as described by Girard et al. [24], to obtain metabolic information about the normal developing white matter (Figure 1).

Conventional MRI—Fetal MRI studies were analyzed by an attending neuroradiologist (RLR) who was blinded to all clinical data. Abnormal patterns of brain development and maturation, and the presence of encephaloclastic lesions, were documented.

Quantitative volumetric MRI analysis—Post-acquisition processing was undertaken on a Linux workstation. MR images of the fetal intracranial cavity were manually masked to extract the fetal brain from the intra-uterine tissue. Each image was corrected for non-

uniformity intensities induced by radio frequency and shading artifacts using the Non-parametric Non-uniform intensity Normalization (N3) tool [25]. In order to minimize the effects of image degradation secondary to fetal motion, an iterative slice-by-slice registration was used, which normalized the intensity of each slice [26]. The middle brain slice, defined as the slice at the mid-point of the brain, was used as a reference, and the global median intensity of each subsequent slice was normalized to the reference using a single scale intensity normalization with a non-linear registration approach. A Gauss-Seidel iterative schema was then applied to register the slices to a weighted average of the considered slice and the two neighboring slices. The rigid-body registration of the slices reached a steady point when it was identical to the previous registration (Figure 2).

After correction for fetal motion, coronal slices were manually segmented using MINC software (www.bic.mni.mcgill.ca/software/minc) to measure intracranial cavity volume (ICV), total brain volume (TBV), and cerebrospinal fluid volume (CSF). ICV included CSF and cerebral, cerebellar, and brainstem parenchymal volumes. TBV included cerebral, cerebellar and brainstem parenchymal volumes but excluded intraventricular and extraventricular CSF (Figure 3). CSF was derived by subtracting TBV from ICV. Volumes were determined by counting the number of voxels in the segmentation, and multiplying by the volume of each voxel; i.e., the volume of each slice equaled the product of slice thickness and the measured coronal area. Total ICV, TBV, and CSF were computed as the sum of volumes measured on each coronal slice.

All measurements were made by a single operator (CL) who was blinded to clinical data. Each coronal area was traced twice, and the average of the two measurements was used for volume calculations. Intra-observer correlation coefficients were determined for measurements of ICV (n=481), TBV (n=458), and CSF (n=481) on all individual slices from 10 MRI studies, and were ≥0.997 in all cases. Intra-observer correlation coefficients were also determined for the summed volumes ICV, TBV, and CSF from 15 MRI scans, and were 0.98 for ICV, 0.96 for TBV, and 0.95 for CSF.

MR spectroscopy analysis—Four metabolites were assessed by ^{1}H-MRS: N-acetyl aspartate (NAA), choline (Cho), creatine (Cr), and lactate. Specifically, NAA, Cho and Cr peaks were identified and measured, and the presence or absence of lactate (identified by an inverted doublet peak around −1.33) was recorded. Cho:Cr and NAA:Cho ratios were calculated when MR spectra satisfied a reliable fit with a standard deviation <20% for each metabolite [27].

Statistical Analysis

The primary hypothesis was that GA- and fetal weight-adjusted TBV in late gestation would be smaller in CHD fetuses than in controls. A secondary hypothesis was that GA- and weight-adjusted measures of cerebral metabolism would be abnormal in CHD fetuses relative to controls. Comparison of demographic and baseline characteristics between cases and controls was performed with chi-square analysis or Wilcoxon rank sum test. To assess for differences in volumetric and ^{1}H-MRS measures between groups, linear regression was performed and models were fit with the appropriate interaction terms and type III sum of squares testing. The equality of regressions was tested between groups using a single F test; comparison of Y-intercepts (25 weeks GA for GA-adjusted analyses) was also performed. Multivariable models were built after consecutive analysis of individual independent variables adjusted for GA and weight percentile. For analysis of each of the volumetric outcomes, independent variables included presence of CHD, CHD diagnostic category (HLHS, TGA or pulmonary atresia, other CHD or control), presence or absence of antegrade flow in the aortic arch, percentage of combined ventricular output through the aortic valve, and cerebral artery flow indices. For

analysis of quantitative metabolic outcomes, the presence of lactate was also included as an independent variable and models were adjusted for GA along with TBV rather than weight percentile. All statistically significant associations are noted. Outcome variables were presented graphically with linear or quadratic curve fitting. In regression models, coefficients of determination (R^2 values) reported in the text reflect the goodness of fit for each independent variable included in the model, or for the complete model if no independent variables were included other than GA and weight percentile (or TBV for metabolic outcomes). Scatterplots are presented with linear or quadratic curve fitting for the groups depicted; R^2 values shown in the figures reflect the goodness of fit for the fitted curve, and not for the adjusted linear regression model. Because MRI studies in control fetuses were typically obtained later in gestation than echocardiograms, echocardiographic data were not included as predictor variables in analyses that included control fetuses, although adjustment was performed using weight percentiles derived from ultrasound estimates of fetal weight.

The authors had full access to the data and take responsibility for its integrity. All authors have read and agree to the manuscript as written.

Results

Subjects

A total of 116 fetuses were enrolled, but 11 were excluded due to excessive fetal motion resulting in inadequate MRI data (n=8), brain dysgenesis (inferior vermian hypoplasia) detected by fetal MRI (n=2, both with CHD), and maternal claustrophobia preventing completion of the MRI (n=1). In the remaining 105 fetuses (50 CHD, 55 controls), MRI was performed at a median GA of 30 weeks (25 1/7 -37 1/7 weeks). Demographic and diagnostic details are summarized in Table 1.

Fetal Echocardiography

Diagnostic data for fetuses with CHD are summarized in Table 1.

Fetal Brain MRI

Conventional MRI analysis—Six fetuses (all with CHD) had mildly abnormal anatomic findings on MRI: 4 with mild (10-13 mm) isolated, unilateral cerebral ventriculomegaly; and 2 with small bilateral subependymal cysts. Data from these fetuses were included in the following analyses.

Quantitative volumetric MRI analysis—Complete volumetric MRI analysis was possible in all 105 fetuses. In control fetuses, there were strong linear relationships between TBV and GA (R^2=0.98, p<0.001), and ICV and GA (R^2=0.96, p<0.001), with progressive increases in TBV and ICV over the third trimester (Figure 4). CSF (R^2=0.80, p<0.001) and the proportion of ICV occupied by CSF (CSF:ICV, R^2=0.93, p<0.001) decreased with increasing GA (Figure 4).

At 25 weeks gestation, TBV and ICV were similar in CHD fetuses and controls (i.e., the 25-week Y-intercept of the control and CHD regression equations did not differ). However, over the third trimester, TBV and ICV were progressively smaller in CHD fetuses relative to controls (p<0.001 for both TBV and ICV; Figure 4). Similar to controls, CSF decreased over the early third-trimester in CHD fetuses, but beyond 30 weeks there was considerable variation. The CSF:ICV ratio, which normally decreases from ~0.4 at 25 weeks to ~0.1 at term, was progressively higher in CHD fetuses through the third trimester (p=0.001) compared with controls (Figure 4). There was no clear difference in TBV between the 6 CHD fetuses with mild abnormalities on conventional MRI and those without.

In a multivariable model adjusted for GA and weight percentile, a lower percentage of combined ventricular output from the aorta ($p<0.001$) and diagnostic category ($p<0.001$) were independently associated with smaller TBV (model $R^2=0.94$).

Similarly, on adjusted multivariable analysis, CHD category was independently associated with the CSF:ICV ratio, with the highest ratios in HLHS and the lowest in fetuses with no CHD or other CHD ($p<0.001$, model $R^2=0.85$).

MR spectroscopy analysis— ^{1}H-MRS spectra were successfully obtained in 75 fetuses, 36 with CHD (72%) and 39 controls (71%). The NAA:Cho ratio increased progressively over the third trimester in controls, from ~0.1 at 25 weeks to ~0.8 at 36 weeks ($R^2=0.94$, $p<0.001$, Figure 5). Compared with controls, NAA:Cho in CHD fetuses was significantly and progressively lower with advancing GA ($p<0.001$) (Figure 5).

On multivariable analysis adjusting for both GA and TBV (a stronger correlate of NAA:Cho than GA), independent predictors of lower NAA:Cho included diagnostic category (HLHS, TGA or pulmonary atresia, other CHD or control; $p<0.001$), absence of antegrade flow in the aortic arch ($p=0.01$), and the presence of lactate ($p<0.001$) (model $R^2=0.90$).

Cho:Cr generally declined over gestation in control (quadratic $R^2=0.47$) and CHD ($R^2=0.23$) fetuses, with relatively weak correlation with GA in both groups. There was no difference in Cho:Cr between cases and controls, and no predictors of Cho:Cr were identified.

Cerebral lactate was detected in 7 of 36 (20%) fetuses with CHD (5 with HLHS, 2 with TGA) between 29 3/7 and 35 5/7 weeks GA. Overall, fetuses with cerebral lactate had the lowest GA- and TBV-adjusted NAA:Cho. No control fetuses had detectable cerebral lactate.

Discussion

Brain Growth and Development in Fetuses with CHD

In this study, we present the first in vivo MRI evidence of abnormal brain volume and metabolism in fetuses with CHD. Compared with normal controls, fetuses with CHD had progressively smaller GA- and weight-adjusted TBV and progressively lower NAA:Cho during the third trimester, a critical developmental period during which there is usually acceleration of energy-demanding brain growth. In addition, we detected cerebral lactate in a subset of fetuses with HLHS and TGA and the lowest adjusted NAA:Cho. Although MRI and ^{1}H-MRS evaluations in this study were cross-sectional, the widening difference between cases and controls in later gestation suggests that there may be progressive impairment of brain growth and maturation in fetuses with CHD, especially in light of the high coefficients of determination for the GA-TBV and GA-NAA:Cho relationships in controls.

These findings add to a growing body of literature detailing antenatal and preoperative neonatal abnormalities of brain size, structure, and function in individuals with CHD [9-19]. Although it is becoming well established that prenatal factors may contribute to the neurodevelopmental morbidity associated with CHD, the specific prenatal causes and mechanisms of insult are largely unknown. Potential mechanisms of abnormal neurologic development in fetuses with CHD include primary genetic and dysgenetic conditions [28,29], secondary disruptions of brain development, and encephaloclastic injury due to acute or chronic oxygen/glucose deprivation [14,30]. Although many critical steps in brain development are completed earlier, major events occur during the second half of gestation, including neuronal migration and arborization, synaptogenesis, programmed cell death, oligodendrocyte maturation, and extensive reorganization of synaptic connections. During the third trimester, there is a surge in synapse formation and activity, with increasing demand for oxygen and metabolic substrate to maintain

Na^+/K^+-ATPase-generated neuronal membrane gradients. Cerebral myelination also accelerates in the third trimester [31,32]. These critical processes in brain development place an escalating demand on the cardiovascular system for delivery of oxygen and energy substrate.

At the outset of this project, one of our underlying hypotheses was that major circulatory disturbances, such as those that occur in complex defects such as HLHS, TGA, and pulmonary atresia, may contribute to abnormal brain development. The basis for this hypothesis was the assumption that circulatory abnormalities in fetuses with these anomalies would place them at risk for inadequate delivery of oxygen and metabolic substrate to the developing brain, slowing normal brain growth and impairing cortical organization and myelination. In the normal fetus, relatively oxygenated umbilical venous return is preferentially directed through the foramen ovale, into the left heart, and out the aortic valve to supply the myocardium and brain [33]. The majority of deoxygenated blood returning from the systemic circulation streams into the right ventricle, through the ductus arteriosus into the descending aorta, and to the placenta (and lower body). In complex CHD, this efficient network may be perturbed, either due to loss or major reduction of outflow from the left or right heart (e.g., HLHS, pulmonary atresia) or to a short-circuit that reverses or eliminates flow streaming (e.g., TGA). Thus, in theory, the content of oxygen and glucose in cerebral arterial blood is likely to be abnormal in fetuses with some forms of complex CHD, although there are no data of which we are aware to support this speculation.

It is not currently feasible to measure oxygen or glucose in human fetal blood. Thus, there is no way to test the proposal that reduced cerebral oxygen and/or glucose delivery contribute to abnormal brain development in fetuses with CHD. Nevertheless, multivariable analysis of factors associated with smaller adjusted TBV and lower NAA:Cho are consistent with the hypothesis that circulatory features contribute to impaired brain development. Specifically, abnormalities of TBV and NAA:Cho were most pronounced in fetuses with HLHS and TGA, and those with a lower percentage of combined ventricular output through the aortic valve or absence of antegrade flow in the aortic arch, and cerebral lactate was found exclusively in the same fetuses. Previous studies have shown cerebral blood flow to be reduced or otherwise abnormal in fetuses or neonates with these anomalies [12,20,21]. Further studies will be necessary to substantiate and elucidate the contribution of cerebral hemodynamics and substrate delivery to abnormal brain development in fetuses with CHD.

Quantitative MRI and MRS in the Evaluation of Brain Development

Quantitative MRI is emerging as a powerful tool for the investigation of early brain development. 3-D MRI in premature infants demonstrated a 4-5 fold increase in the volumes of cerebral cortical gray and myelinated white matter between 28-40 weeks post-conception, as well as an association between volumetric abnormalities and adverse neurodevelopmental outcome [34,35].

Similarly, ^{1}H-MRS may offer insight into brain development in high-risk neonates and fetuses. NAA increases with GA and decreases with brain injury [24], and reflects not only the development of dendrites and synapses but also oligodendrocyte proliferation and differentiation [36]. Both NAA and lactate reflect neuronal mitochondrial function, and may be valuable measures of brain metabolism [37,38]. Cerebral lactate, a marker of anaerobic metabolism in the newborn and fetus [38,39], has been found in up to 50% of preoperative infants with CHD [14,15] and is associated with adverse outcome in other high-risk infants [40]. Although lactate has been identified with ^{1}H-MRS in stable premature infants, it has not been reported in normal fetuses [24,41]. Longitudinal evaluation of the fetuses in this study should help elucidate the clinical significance of cerebral NAA:Cho and lactate in fetuses with complex CHD.

Limitations

Recently reported multislice snapshot image techniques that may provide higher resolution imaging of the fetal brain than the acquisitions used in this study [42]. These acquisitions were not available at the beginning of this study and were not incorporated into our fetal MRI protocol. Although we attempted to exclude fetuses with genetic and/or cerebral dysgenetic conditions, undiagnosed or as yet unknown genetic conditions may have been missed. Such anomalies may be more common in subjects with CHD than in controls, potentially introducing bias. The temporal relationship between fetal MRI and echocardiograms differed between control and CHD groups; therefore, comparison of cardiovascular parameters was not possible between these groups. Finally, we did not measure serial fetal brain volumes and therefore could not truly assess growth. Follow-up MRI studies are underway in this cohort, measuring neonatal brain volume and metabolism prior to cardiac surgery.

Conclusions

Brain volume and metabolism are abnormal in third-trimester fetuses with some forms of complex CHD, particularly those with HLHS or TGA, and reduced flow through the systemic ventricle or antegrade around the aortic arch. Quantitative MRI may provide deeper insight into the timing of insults that might disrupt normal fetal brain development. Although further studies are needed to confirm and elucidate these findings, the data presented in this report offer promise that quantitative MRI will advance our understanding of the neurodevelopmental implications of circulatory pathophysiology, extend our ability to provide informed parental counseling, and aid in evaluating the neurodevelopmental impact of prenatal intervention.

Acknowledgments

We thank the American Heart Association for recognizing this work at their 2008 annual meeting with the Outstanding Research Award in Pediatric Cardiology (C. Limperopoulos). We thank Yansong Zhao for assistance with MRI applications, Helene Hakyemez for assistance with MRI data processing, and Shaye Moore for assistance with manuscript preparation. We are indebted to the families for participating in this study.

Funding Sources: This work was supported by the Canadian Institutes of Health Research (MOP-81116), Sickkids Foundation (XG 06-069), Canada Research Chairs Program (Dr. Limperopoulos), NIH National Institute of Neurological Disorders and Stroke (K24NS057568), the Trust Family Foundation, and the Farb Family Fund.

Abbreviations

CHD	congenital heart disease
MRI	magnetic resonance imaging
^{1}H-MRS	proton magnetic resonance spectroscopy
GA	gestational age
HLHS	hypoplastic left heart syndrome
TGA	transposition of the great arteries
ICV	intracranial cavity volume
TBV	total brain volume
CSF	cerebrospinal fluid volume
NAA	N-acetyl aspartate
Cho	choline
Cr	creatine

References

1. Dittrich H, Buhrer C, Grimmer I, Dittrich S, Abdul-Khaliq H, Lange PE. Neurodevelopment at 1 year of age in infants with congenital heart disease. Heart 2003;89:436–41. [PubMed: 12639876]
2. Tabbutt S, Nord AS, Jarvik GP, Bernbaum J, Wernovsky G, Gerdes M, Zackai E, Clancy RR, Nicolson SC, Spray TL, Gaynor JW. Neurodevelopmental outcomes after staged palliation for hypoplastic left heart syndrome. Pediatrics 2008;121:476–83. [PubMed: 18310195]
3. Massaro AN, El-Dib M, Glass P, Aly H. Factors associated with adverse neurodevelopmental outcomes in infants with congenital heart disease. Brain Dev 2008;30:437–46. [PubMed: 18249516]
4. Ballweg JA, Wernovsky G, Gaynor JW. Neurodevelopmental outcomes following congenital heart surgery. Pediatr Cardiol 2007;28:126–33. [PubMed: 17265108]
5. Newburger JW, Jonas RA, Wernovsky G, Wypij D, Hickey PR, Kuban KCK, Farrell DM, Holmes GL, Helmers SL, Constantinou J, Carrazana E, Barlow JK, Walsh AZ, Lucius KC, Share JC, Wessel DL, Hanley FL, Mayer JE, Castaneda AR, Ware JH. A comparison of the perioperative neurologic effects of hypothermic circulatory arrest versus low-flow cardiopulmonary bypass in infant heart surgery. N Eng J Med 1993;329:1057–64.
6. Jonas RA, Wypij D, Roth SJ, Bellinger DC, Visconti KJ, du Plessis AJ, Goodkin H, Laussen PC, Farrell DM, Bartlett J, McGrath E, Rappaport LJ, Bacha EA, Forbess JM, del Nido PJ, Mayer JE Jr, Newburger JW. The influence of hemodilution on outcome after hypothermic cardiopulmonary bypass: results of a randomized trial in infants. J Thorac Cardiovasc Surg 2003;126:1765–74. [PubMed: 14688685]
7. Newburger JW, Jonas RA, Soul J, Kussman BD, Bellinger DC, Laussen PC, Robertson R, Mayer JE Jr, del Nido PJ, Bacha EA, Forbess JM, Pigula F, Roth SJ, Visconti KJ, du Plessis AJ, Farrell DM, McGrath E, Rappaport LA, Wypij D. Randomized trial of hematocrit 25% versus 35% during hypothermic cardiopulmonary bypass in infant heart surgery. J Thorac Cardiovasc Surg 2008;135:347–54. [PubMed: 18242267]
8. Clancy RR, McGaurn SA, Goin JE, Hirtz DG, Norwood WI, Gaynor JW, Jacobs ML, Wernovsky G, Mahle WT, Murphy JD, Nicolson SC, Steven JM, Spray TL. Allopurinol neurocardiac protection trial in infants undergoing heart surgery using deep hypothermic circulatory arrest. Pediatrics 2001;108:61–70. [PubMed: 11433055]
9. Limperopoulos C, Majnemer A, Rosenblatt B, Shevell M, Rohlicek C, Tchervenkov C. Multimodality evoked potential findings in infants with congenital heart defects. J Child Neurol 1999;14:702–7. [PubMed: 10593545]
10. Limperopoulos C, Majnemer A, Shevell MI, Rosenblatt B, Rohlicek C, Tchervenkov C. Neurodevelopmental status of newborns and infants with congenital heart defects before and after open heart surgery. J Pediatr 2000;137:638–45. [PubMed: 11060529]
11. Limperopoulos C, Majnemer A, Rosenblatt B, Shevell MI, Rohlicek C, Tchervenkov C, Gottesman R. Association between electroencephalographic findings and neurologic status in infants with congenital heart defects. J Child Neurol 2001;16:471–6. [PubMed: 11453441]
12. Licht DJ, Wang J, Silvestre DW, Nicolson SC, Montenegro LM, Wernovsky G, Tabbutt S, Durning SM, Shera DM, Gaynor JW, Spray TL, Clancy RR, Zimmerman RA, Detre JA. Preoperative cerebral blood flow is diminished in neonates with severe congenital heart defects. J Thorac Cardiovasc Surg 2004;128:841–9. [PubMed: 15573068]
13. Te Pas AB, van Wezel-Meijler G, Bokenkamp-Gramann R, Walther FJ. Preoperative cranial ultrasound findings in infants with major congenital heart disease. Acta Paediatr 2005;94:1597–603. [PubMed: 16352496]
14. Mahle WT, Tavani F, Zimmerman RA, Nicolson SC, Galli KK, Gaynor JW, Clancy RR, Montenegro LM, Spray TL, Chiavacci RM, Wernovsky G, Kurth CD. An MRI study of neurological injury before and after congenital heart surgery. Circulation 2002;106:I109–14. [PubMed: 12354718]
15. Miller SP, McQuillen PS, Hamrick S, Xu D, Glidden DV, Charlton N, Karl T, Azakie A, Ferriero DM, Barkovich AJ, Vigneron DB. Abnormal brain development in newborns with congenital heart disease. N Engl J Med 2007;357:1928–38. [PubMed: 17989385]
16. Hinton RB, Andelfinger G, Sekar P, Hinton AC, Gendron RL, Michelfelder EC, Robitaille Y, Benson DW. Prenatal head growth and white matter injury in hypoplastic left heart syndrome. Pediatr Res 2008 2008;64:364–9.

17. Licht DJ, Shera DM, Clancy RR, Wernovsky G, Montenegro LM, Nicolson SC, Zimmerman RA, Spray TL, Gaynor JW, Vossough A. Brain maturation is delayed in infants with complex congenital heart defects. J Thorac Cardiovasc Surg 2009;137:529–36. [PubMed: 19258059]
18. Limperopoulos C, Majnemer A, Shevell MI, Rohlicek C, Rosenblatt B, Tchervenkov C, Darwish HZ. Predictors of developmental disabilities after open heart surgery in young children with congenital heart defects. J Pediatr 2002;141:51–8. [PubMed: 12091851]
19. Majnemer A, Limperopoulos C, Shevell M, Rosenblatt B, Rohlicek C, Tchervenkov C. Long-term neuromotor outcome at school entry of infants with congenital heart defects requiring open-heart surgery. J Pediatr 2006;148:72–7. [PubMed: 16423601]
20. Donofrio MT, Bremer YA, Schieken RM, Gennings C, Morton LD, Eidem BW, Cetta F, Falkensammer CB, Huhta JC, Kleinman CS. Autoregulation of cerebral blood flow in fetuses with congenital heart disease: the brain sparing effect. Pediatr Cardiol 2003;24:436–43. [PubMed: 14627309]
21. Kaltman JR, Di H, Tian Z, Rychik J. Impact of congenital heart disease on cerebrovascular blood flow dynamics in the fetus. Ultrasound Obstet Gynecol 2005;25:32–6. [PubMed: 15593334]
22. Hadlock FP, Harrist RB, Carpenter RJ, Deter RL, Park SK. Sonographic estimation of fetal weight. The value of femur length in addition to head and abdomen measurements. Radiology 1984;150:535–40. [PubMed: 6691115]
23. Doubilet PM, Benson CB, Nadel AS, Ringer SA. Improved birth weight table for neonates developed from gestations dated by early ultrasonography. J Ultrasound Med 1997;16:241–9. [PubMed: 9315150]
24. Girard N, Gouny SC, Viola A, Le Fur Y, Viout P, Chaumoitre K, D'Ercole C, Gire C, Figarella-Branger D, Cozzone PJ. Assessment of normal fetal brain maturation in utero by proton magnetic resonance spectroscopy. Magn Reson Med 2006;56:768–75. [PubMed: 16964617]
25. Sled JG, Zijdenbos AP, Evans AC. A nonparametric method for automatic correction of intensity nonuniformity in MRI data. IEEE Trans Med Imaging 1998;17:87–97. [PubMed: 9617910]
26. Guizard, N.; Lepag, C.; Fonov, V.; Hakyemez, H.; Evans, A.; Limperopoulos, C. Development of a fetal brain atlas from multi-axial MR acquisitions. Proceedings, 16th Scientific Meeting, International Society for Magnetic Resonance in Medicine; Toronto. 2008. p. 132
27. Kok RD, van den Berg PP, van den Bergh AJ, Nijland R, Heerschap A. Maturation of the human fetal brain as observed by 1H MR spectroscopy. Magn Reson Med 2002;48:611–6. [PubMed: 12353277]
28. Glauser T, Rorke L, Weinberg P, Clancy R. Congenital brain anomalies associated with the hypoplastic left heart syndrome. Pediatrics 1990;85:984–90. [PubMed: 2339047]
29. Andelfinger G. Genetic factors in congenital heart malformation. Clin Genet 2008;73:516–27. [PubMed: 18462450]
30. Petit CJ, Rome JJ, Wernovsky G, Mason SE, Shera DM, Nicolson SC, Montenegro LM, Tabbutt S, Zimmerman RA, Licht DJ. Preoperative brain injury in transposition of the great arteries is associated with oxygenation and time to surgery, not balloon atrial septostomy. Circulation 2009;119:709–16. [PubMed: 19171858]
31. Brody BA, Kinney HC, Kloman AS, Gilles FH. Sequence of central nervous system myelination in human infancy. I. An autopsy study of myelination. J Neuropathol Exp Neurol 1987;46:283–301. [PubMed: 3559630]
32. Huppi PS, Warfield S, Kikinis R, Barnes PD, Zientara GP, Jolesz FA, Tsuji MK, Volpe JJ. Quantitative magnetic resonance imaging of brain development in premature and mature newborns. Ann Neurol 1998;43:224–35. [PubMed: 9485064]
33. Edelstone DI, Rudolph AM. Preferential streaming of ductus venosus blood to the brain and heart in fetal lambs. Am J Physiol 1979;237:724–9.
34. Peterson BS, Vohr B, Staib LH, Cannistraci CJ, Dolberg A, Schneider KC, Katz KH, Westerveld M, Sparrow S, Anderson AW, Duncan CC, Makuch RW, Gore JC, Ment LR. Regional brain volume abnormalities and long-term cognitive outcome in preterm infants. JAMA 2000;284:1939–47. [PubMed: 11035890]
35. Tolsa CB, Zimine S, Warfield SK, Freschi M, Sancho Rossignol A, Lazeyras F, Hanquinet S, Pfizenmaier M, Huppi PS. Early alteration of structural and functional brain development in

premature infants born with intrauterine growth restriction. Pediatr Res 2004;56:132–8. [PubMed: 15128927]

36. Bhakoo KK, Pearce D. In vitro expression of N-acetyl aspartate by oligodendrocytes: implications for proton magnetic resonance spectroscopy signal in vivo. J Neurochem 2000;74:254–62. [PubMed: 10617127]
37. Demougeot C, Garnier P, Mossiat C, Bertrand N, Giroud M, Beley A, Marie C. N-Acetylaspartate, a marker of both cellular dysfunction and neuronal loss: its relevance to studies of acute brain injury. J Neurochem 2001;77:408–15. [PubMed: 11299303]
38. Azpurua H, Alvarado A, Mayobre F, Salom T, Copel JA, Guevara-Zuloaga F. Metabolic assessment of the brain using proton magnetic resonance spectroscopy in a growth-restricted human fetus: case report. Am J Perinatol 2008;25:305–9. [PubMed: 18437645]
39. Wolfberg AJ, Robinson JN, Mulkern R, Rybicki F, Du Plessis AJ. Identification of fetal cerebral lactate using magnetic resonance spectroscopy. Am J Obstet Gynecol 2007;196:e9–11. [PubMed: 17240215]
40. Barkovich AJ, Baranski K, Vigneron D, Partridge JC, Hallam DK, Hajnal BL, Ferriero DM. Proton MR spectroscopy for the evaluation of brain injury in asphyxiated, term neonates. AJNR Am J Neuroradiol 1999;20:1399–405. [PubMed: 10512219]
41. Girard N, Fogliarini C, Viola A, Confort-Gouny S, Fur YL, Viout P, Chapon F, Levrier O, Cozzone P. MRS of normal and impaired fetal brain development. Eur J Radiol 2006;57:217–25. [PubMed: 16387464]
42. Jiang S, Xue H, Glover A, Rutherford M, Rueckert D, Hajnal JV. MRI of moving subjects using multislice snapshot images with volume reconstruction (SVR): application to fetal, neonatal, and adult brain studies. IEEE Trans Med Imaging 2007;26:967–80. [PubMed: 17649910]

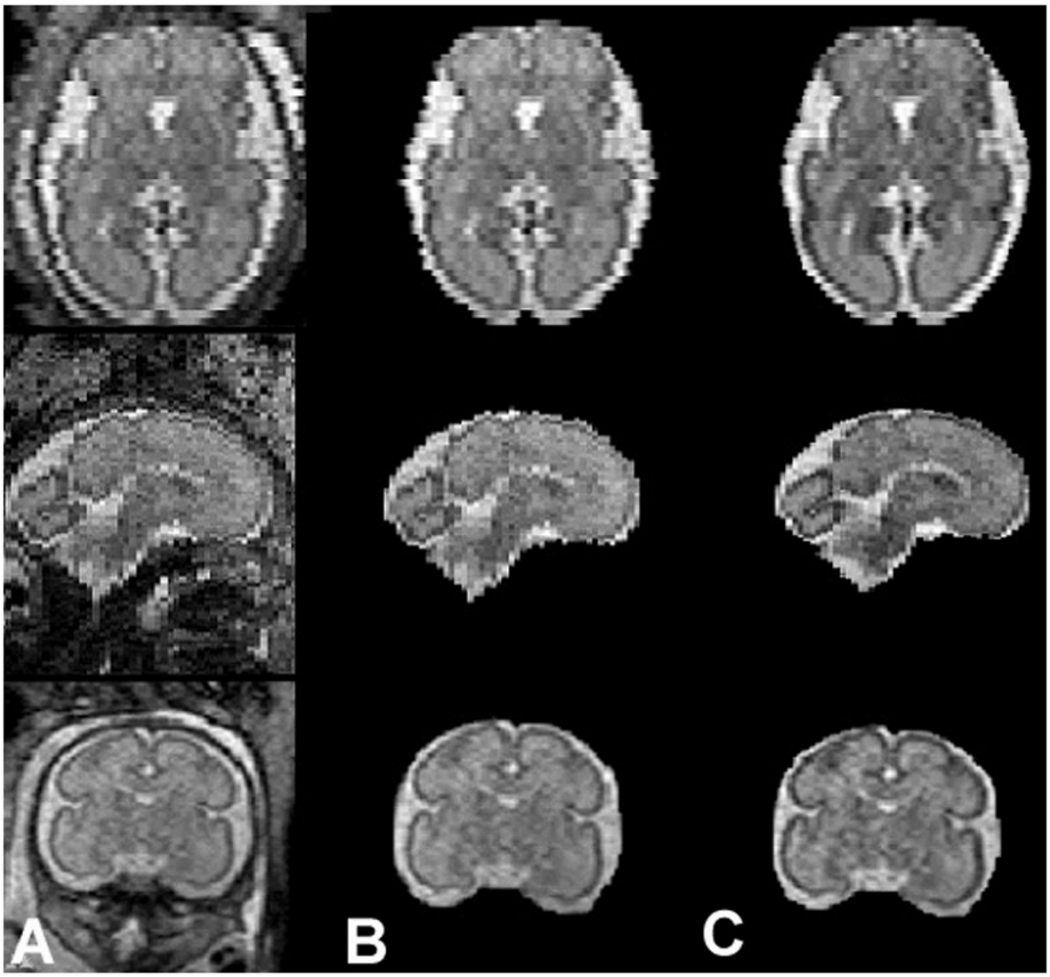

Figure 1.
Fetal MR image reconstruction. Raw fetal MRI images (column A), fetal intracranial cavity extraction (column B), and fetal MRI images following intensity correction and slice alignment (column C).

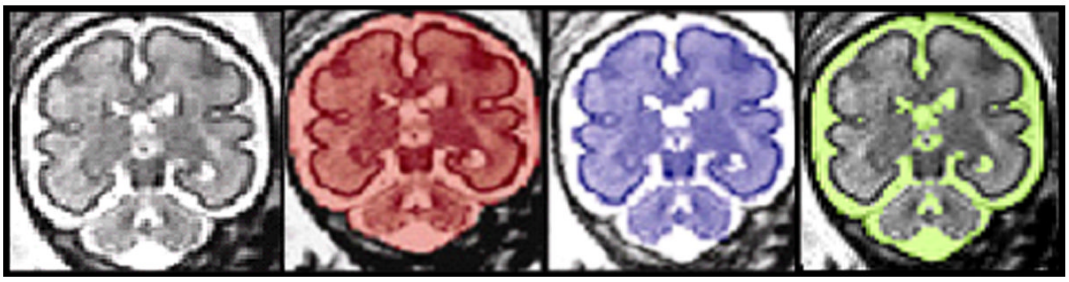

Figure 2.
Manual segmentation of Fetal MR coronal images. 3-D manual segmentation of intracranial cavity volume (red), total brain volume (blue) and cerebral spinal fluid (yellow) using coronal images.

Figure 3.
In fetal MRS, the voxel of interest was placed in the cerebral hemisphere at the level of the centrum ovale.

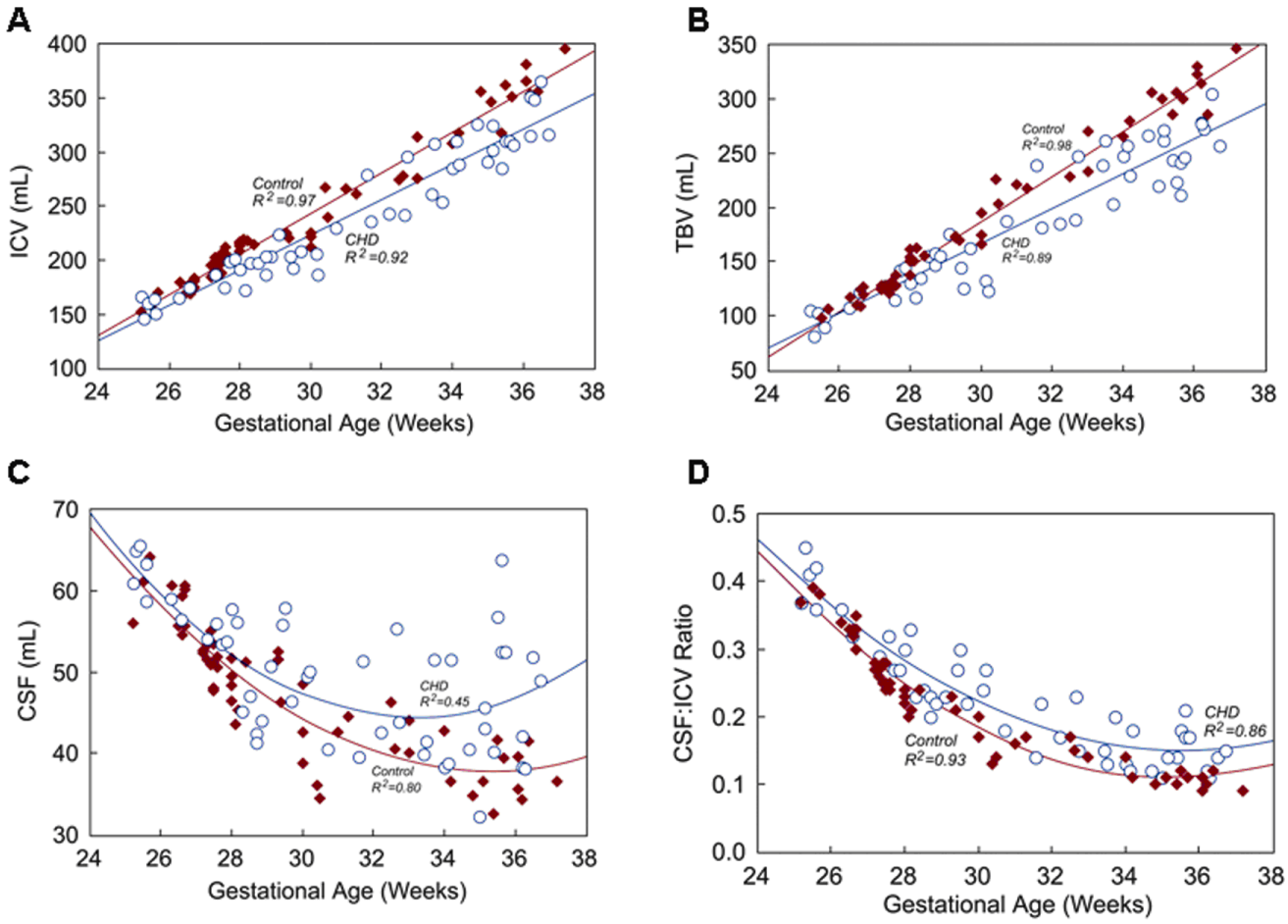

Figure 4.

Relationships between GA and A) ICV, B) TBV, C) CSF, and D) CSF:ICV in fetuses with CHD (open blue circles) and normal control fetuses (solid red diamonds). Regression equations for fetuses with CHD and controls are: A) ICV CHD = (16.272 × GA) − 265.04, ICV control = (18.744 × GA) − 319.20; B) TBV CHD = (16.081 × GA) − 315.78, TBV control = (20.886 × GA) − 439.41; C) CSF CHD = (0.30052 × GA^2) + (-19.936 × GA) + 374.92, CSF control = (0.23769 × GA^2) + (-16.768 × GA) + 333.42; D) CSF:ICV CHD = (0.002308 × GA^2) + (-0.16478 × GA) + 3.0873, CSF:ICV control = (0.002534 × GA^2) + (-0.17985 × GA) + 3.2988. The depicted R^2 values reflect the goodness of fit for the fitted curve for each group, and not for the adjusted linear regression model.

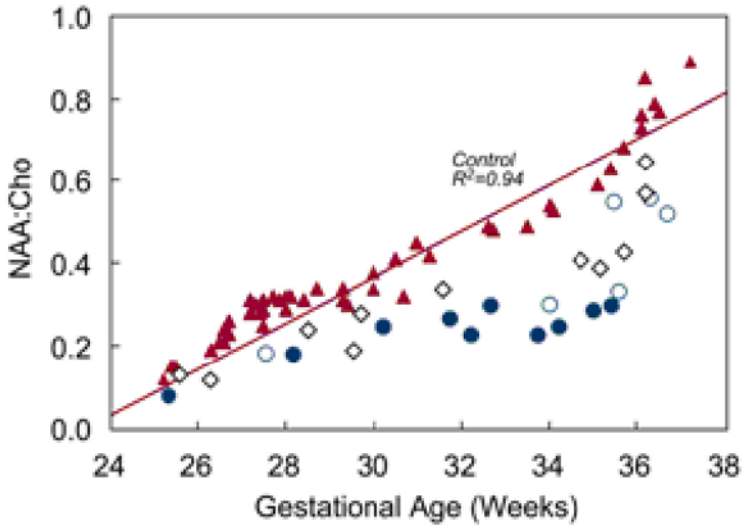

Figure 5.

Relationship between NAA:Cho and GA according to diagnosis. Fetuses with HLHS are indicated with blue circles (those with absence of antegrade blood flow in the transverse aortic arch are solid and others are open), fetuses with TGA or pulmonary atresia are indicated by the open black diamonds, and control fetuses and fetuses with other forms of CHD are indicated by the red triangles.

Table 1

Characteristics of the cohort (N = 105)

Characteristic	Subjects with CHD N=50	Controls N=55	P value*
Male; n (%)	32 (64%)	32 (58%)	0.60
Weight percentile at echocardiography	65 (8-99)	58 (3-95)	0.59
Median (range) gestational age at MRI (weeks)	31 (25 1/7 - 365/7)	28 (25 1/7 - 37 1/7)	0.06
Duration between MRI and echocardiography			
Median (range) days	0 (0-41)	49 (0-125)	<0.001
n (%) of subjects within 1 day	36 (72%)	6 (11%)	<0.001
n (%) of subjects within 10 days	46 (92%)	6 (11%)	<0.001
Type of CHD; n (%)			
Hypoplastic left heart syndrome	19 (38%)		
Transposition of the great arteries	13 (26%)		
Pulmonary atresia with intact ventricular septum	7 (14%)		
Other			
Tetralogy of Fallot/double-outlet right ventricle	4 (8%)		
Valvar pulmonary stenosis	3 (6%)		
Truncus arteriosus	1 (2%)		
Ebstein's malformation	1 (2%)		
Tricuspid atresia	1 (2%)		
Aortic stenosis	1 (2%)		
Selected physiologic variables			
Percentage of combined ventricular output through the aortic valve	40 (0-100)		
Antegrade flow in the aortic arch	37 (74%)		

Data are presented as number (%) or median (range)

* By chi-square analysis or Wilcoxon rank sum test